

# The effect of asymmetries on non-neutral plasma confinement time

J. Notte and J. Fajans

Department of Physics, University of California, Berkeley, California 94720

(Received 15 November 1993; accepted 10 January 1994)

Theory predicts that perfectly azimuthally symmetric non-neutral plasma traps should confine plasma forever. Unintentional trap asymmetries are believed to limit plasma confinement times to less than  $< 10^5$  s. Deliberately applied electrostatic fields break the azimuthal symmetry and affect the plasma confinement time. While small, deliberate asymmetries do not significantly reduce the trap's confinement properties, large asymmetries significantly degrade the plasma confinement. The scaling laws of this degradation are studied herein. The mechanism of plasma loss appears to change when deliberate asymmetries are applied.

## I. INTRODUCTION

Pure electron plasmas<sup>1,2</sup> are frequently confined in the simple geometry shown in Fig. 1. The plasma is trapped in the middle of a set of three collimated cylinders. Negative potentials applied to the two adjacent cylinders assure confinement in the axial direction. A strong magnetic field, aligned parallel to the trap's axis of symmetry, inhibits the radial transport of the plasma. More complete descriptions of this type of pure electron plasma trap can be found in the literature.<sup>1</sup> These traps can also confine pure ion plasmas and positron plasmas.<sup>3-5</sup>

In his paper on the non-neutral plasma confinement theorem,<sup>6</sup> O'Neil derives an upper bound on the allowed expansion of a plasma held in an azimuthally symmetric trap. The theorem follows from the fact that the canonical angular momentum of the electrons is the sum of the electron's magnetic angular momentum ( $\mathbf{r}_i \times e\mathbf{A}/c$ ) and the electron's mechanical angular momentum ( $\mathbf{r}_i \times \mathbf{p}_i$ ). [Here we use  $\mathbf{A} = (Br/2)\hat{\theta}$  for the vector potential of a uniform solenoidal magnetic field of strength  $B$ , and  $r_i$  to denote the radial position of the  $i$ th electron.] For the plasma parameters considered here, the magnetic angular momentum term is much larger than the mechanical angular momentum term. Thus the total angular momentum is approximately proportional to the summed squared radial positions of the electrons,  $L_{\text{total}} \propto \sum r_i^2$ . Since an azimuthally symmetric trap cannot exert a net torque on the plasma, the quantity  $\sum r_i^2$  must remain constant. This invariance bounds the radial expansion of the plasma because, if some electrons approach the walls and are lost, the remainder must move closer to the center of the trap. This confinement theorem is rendered inapplicable in the presence of azimuthal asymmetries because such asymmetries can apply torques. However, we expect that small asymmetries will induce only slow changes in angular momentum, and correspondingly small rates of plasma expansion.

Since azimuthal asymmetries degrade the plasma lifetime, these asymmetries are minimized during trap construction by carefully machining the trap cylinders and by accurately aligning them with the trap magnetic field. Nonetheless, unavoidable residual asymmetries cause gradual plasma expansion. The plasma "lifetime" is traditionally denoted by  $\tau_m$ , and is defined to be the time required

for the plasma's central density,  $n_c$ , to be reduced to half of its original value. The scaling of  $\tau_m$  with trap parameters and plasma parameters has been documented previously.<sup>7-9</sup> Certain traps obtain plasma lifetimes as long as  $10^5$  s.

We find that deliberately applied electrostatic asymmetries do not cause instantaneous plasma loss. We introduce these asymmetries by applying nonzero voltages to a patch on the cylindrical wall. Shown at the top of the middle cylinder in Fig. 1, this wall patch is electrically isolated, but otherwise coincident with the surrounding cylindrical wall. With the perturbation applied along the full axial length of the plasma, the plasma assumes an asymmetric equilibrium shape which has been studied extensively.<sup>10,11</sup> The existence of these confined, asymmetric plasmas motivates the research presented here. However, we study the more general case in which the axial length of the wall patch is short compared to the plasma's length. Experiments with deliberately applied asymmetries may provide some insight into how asymmetries in general (including asymmetries resulting from imperfect construction) affect nonneutral plasma confinement times.

In Sec. II, the general procedures followed in the experiments reported here are described. We define  $\tau_m^a$  to be the time for the plasma's central density to be reduced by a factor of 2 in the presence of an applied asymmetry, and, in Sec. III, we vary the strength of the applied perturbation to determine its effect on  $\tau_m^a$ . Also studied in this section is the effect of combining multiple perturbations. In Secs. IV-VII, the plasma density, temperature, length, and the confining magnetic field are varied independently to determine the scaling of  $\tau_m^a$ . The general form by which  $n_c$  decays over time, and how this is changed by the application of perturbations is discussed in the Appendix.

## II. EXPERIMENTAL PROCEDURE

The trap is operated with repeated cycles of inject, hold, and dump phases. During the inject phase the leftmost cylinder in Fig. 1 is momentarily grounded, allowing electrons to flow from the hot tungsten filament to the center of the trap. This cylinder is then biased negatively to trap the plasma in the center cylinder. Next, during the hold phase, the plasma is held for a variable length of time. The asymmetry is applied at the start of this phase by

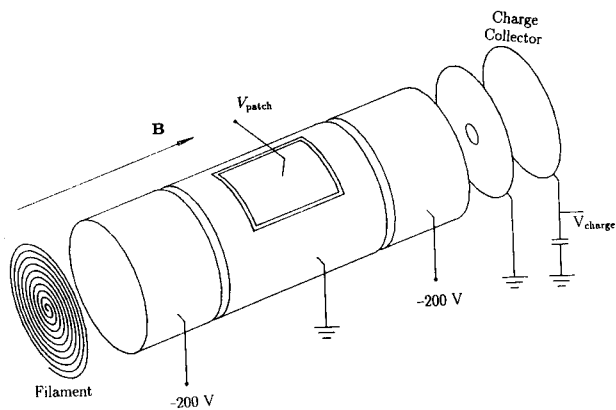


FIG. 1. Confinement geometry for pure electron plasmas.

slowly (slowly compared to the plasma self rotation frequency<sup>12,10</sup>) ramping up the perturbing voltage,  $V_p$ , on the electrically isolated wall patch. The patch has an angular width of  $50^\circ$ , a length of 2.54 cm and is coincident with the cylindrical wall radius of 1.095 cm. The perturbation is slowly removed at the end of the hold period, so the plasma reassumes a cylindrically symmetric shape with a well-defined center. Finally, during the dump phase, the plasma is allowed to flow out of the trap along the magnetic field lines. The plasma's central density is obtained from the charge which passes through a small, centered hole and onto a charge collector. The confinement time,  $\tau_m^a$ , of these perturbed plasmas is determined from the decay of the plasma's central density with time,  $n_c(t)$ .

The experiments are complicated by the presence of an instability<sup>13-15</sup> which causes the  $l=1$  diocotron mode to grow slowly. This instability is suppressed by intermittently applying active feedback between two additional wall patches to damp away this mode.<sup>16,17</sup> Since the feedback is enabled for a duty cycle of less than 1%, and since the amplitude is kept to a minimum, the feedback has little effect on the plasma expansion.

We begin by determining the scaling of plasma confinement time with patch voltage,  $\tau_m^a(V_p)$ , for a single set of plasma parameters: magnetic field  $B=500$  G; plasma density  $n_p=1 \times 10^7$  cm<sup>-3</sup>; temperature  $T \approx 1.6$  eV; plasma length  $L_p \approx 10$  cm; and plasma radius  $r_p \approx 1.0$  cm. We then determine the scaling of  $\tau_m^a$  as each parameter is varied independently. The experiment actually consists of many more than the three cylinders shown in Fig. 1; the plasma length is varied by using additional grounded cylinders between the two negatively biased end cylinders. While these experiments include a range of plasma lengths, the center of the wall patch is always 2.2 cm from one of the negative confining cylinders.

### III. SCALING WITH PERTURBATION STRENGTH

The observed scaling of the confinement time  $\tau_m^a$  with the size of the applied asymmetry  $V_p$  is seen in Fig. 2. Note that the longest confinement time is obtained for the non-zero perturbation,  $V_p=1.0 \pm 0.2$  V, suggesting that the unknown mechanism for plasma loss in the symmetric case

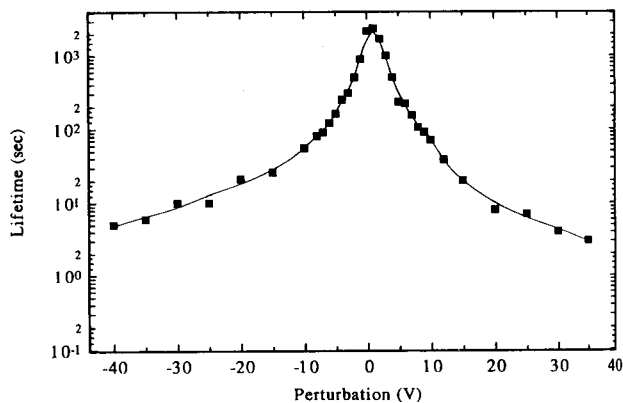


FIG. 2. The effect of a patch bias on plasma confinement.

can be inhibited by an applied perturbation. This possibility has been explored by Eggleston,<sup>18</sup> who reports that an elaborate set of applied perturbations can improve the confinement time by up to 40%.

Away from the central peak, the confinement is degraded with increasing magnitude of  $V_p$ . As shown in Fig. 3, this data is well described by a relation of the form,  $\tau_m^a \propto |V_p|^m$ . For this set of data, the best fit for the positive perturbations has a slope,  $m_+ = -2.14 \pm 0.08$ , while the best fit for negative perturbations has a slope,  $m_- = -1.72 \pm 0.05$ . For other plasma parameters, we find that this slope varies by up to 20%, but is always near  $-2$ , and that positive perturbations consistently have a larger slope.

The stronger influence of positive perturbations on confinement time may be explained in terms of an uneven longitudinal distribution of electrons along a given magnetic-field line. Since the wall patch is short compared to the plasma length, a positive perturbation will cause an excess of electrons to collect near the wall patch. Similarly, fewer electrons are located near a negatively biased wall patch, so the perturbation has a lesser ability to degrade plasma confinement.

We have omitted from these graphs data points that correspond to very large positive and negative perturbations. Past a certain point, larger perturbations result in a slight increase in confinement time, compared to measure-

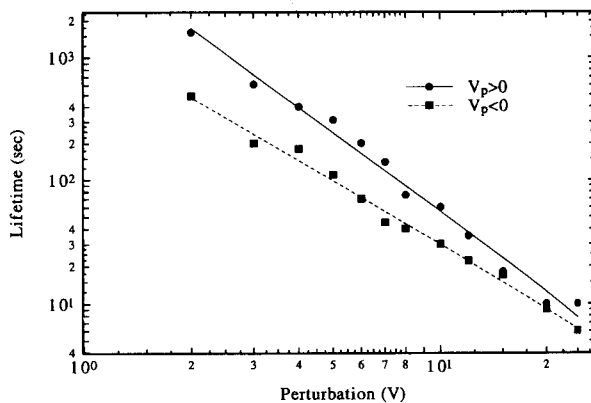


FIG. 3. Scaling of confinement time with perturbation.

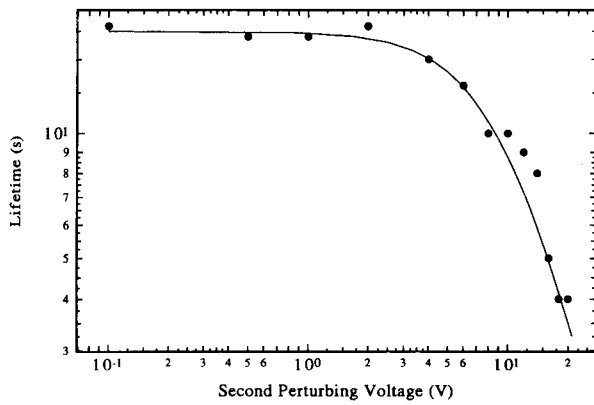


FIG. 4. The combination of two unequal perturbations.

ments made below this point. Depending on the sign of the perturbation, such perturbations either axially trap the plasma near the patch, or repel it away from the patch. Either way, the plasma is effectively shorter, and it is well documented<sup>9</sup> that shorter plasmas can be confined for longer times. The point at which this anomalous behavior sets in depends on the plasma density, and length. In practice, a full scan over  $V_p$  is made, and data which exhibit this anomalously improved confinement for large perturbations is discarded. The hypothesis that the plasma is longitudinally trapped near the patch for large positive perturbations has been verified by maintaining the positive bias on the patch during the dump. Under these circumstances, little or no plasma is dumped since it is trapped in the well created by the patch.

The degradation of plasma lifetime which results from multiple perturbations has also been studied. Applying the same bias to two wall patches reduces the confinement time to 60% of the confinement time for the same bias on just one patch. The two patches have the same axial position and length, but are separated by 90° in the azimuthal direction. Presumably, this factor (60%) is dependent upon the geometry of the wall patches. Varying one patch ( $V_{p2}$ ) while keeping the other patch at a constant bias of  $V_{p1} = 10$  V more clearly reveals how multiple perturbations combine. Figure 4 shows that this data conforms to the expected limiting cases for small ( $\tau_m^a = \text{const}$ ) and large ( $\tau_m^a \propto V_{p2}^{-2}$ ) patch voltages. The solid line in the graph represents the simplest possible model for adding these perturbations,  $\tau_m^a \propto (V_{p1}^2 + V_{p2}^2)^{-1}$ , consistent with producing the correct asymptotic forms. However, the agreement is not so convincing as to rule out other models.

The confinement theorem implies that the plasma lifetime is determined by some combination of applied and inherent asymmetries. If the asymmetries can be treated on an equal footing,<sup>19</sup> then a measure of the trap's construction asymmetry can be translated into a perturbing voltage,  $V_t$ . With this assumption, the simplest model for the plasma confinement time is

$$\tau_m^a \propto (V_p^2 + V_t^2)^{-1}. \quad (1)$$

This model is consistent with O'Neil's confinement

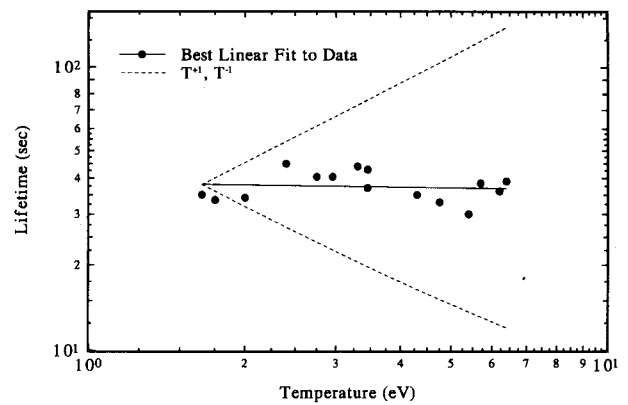


FIG. 5. Temperature dependence of asymmetric plasma confinement time.

theorem,<sup>6</sup> in that it predicts an infinite confinement time for perfectly symmetric traps. This model also approaches the correct limiting form for large  $V_p$ . A measure of our trap's intrinsic asymmetry can be inferred from the full width at half maximum of Fig. 2, yielding  $V_t \approx 3$  V. If a bias of 3 V were applied to a wall patch, it would displace the outermost equipotentials by about 0.2 cm. An equivalent distortion of the equipotentials would result from a cylinder with a 0.2 cm dent on one side. This represents a very large asymmetry (10% of the cylinder radius) and it is unlikely that the construction or alignment errors could be responsible. For comparison, the confining cylinders were machined to a tolerance of  $\pm 0.001$  cm.

#### IV. PLASMA TEMPERATURE SCALING

The confinement of these asymmetric plasmas is relatively independent of the initial plasma temperature. The plasma can be heated by subjecting it to a 700 kHz square wave applied to a wall patch for 3 ms. Initial plasma temperatures ranging from 1.6 to 6.4 eV can be obtained by varying the amplitude of this square wave from 0 to 7 V. Figure 5 shows that  $\tau_m^a$  is relatively independent of plasma temperature for  $V_p = 10$  V. For contrast, two hypothetical scaling laws are also shown in this figure. Note that the plasma temperature will not necessarily remain constant throughout the confinement time. Additional plasma heating occurs because the plasma expands towards the wall,<sup>8</sup> converting some of its electrostatic energy to thermal kinetic energy as it does so. The plasma also cools by collisions with the room temperature background neutrals. In our experiments the cooling process dominates, yielding a measured cooling time scale of  $\sim 50$  s.

#### V. PLASMA DENSITY SCALING

The plasma density can be varied by splitting the initial plasma into two axial parts, one of which is discarded. The remaining plasma is then expanded to its original length, reducing its density and temperature. The plasma cooling which occurs during this chopping procedure is assumed to be unimportant because, as shown above,  $\tau_m^a$  is relatively

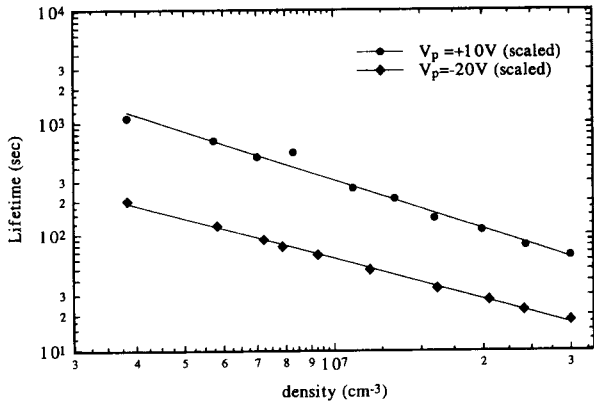


FIG. 6. Density dependence of asymmetric plasma confinement time.

independent of temperature. The usual  $\tau_m^a \propto V_p^{-2}$  behavior is observed for both high- and low-density plasmas.

For a given  $V_p$ , low-density plasmas will be more distorted than high-density plasmas. This effect, which arises from the proportionality of charge and potential, is expected and uninteresting. Consequently, we remove this effect by scaling the perturbation strength with plasma density. This scaling serves to keep the plasma shape the same while the density is varied. For example, to compare a plasma with  $n_p = 3 \times 10^7 \text{ cm}^{-3}$ , distorted by a perturbation  $V_p = +15 \text{ V}$ , with a lower-density plasma with  $n_p = 1 \times 10^7 \text{ cm}^{-3}$ , we scale the perturbation to  $V_p = +5 \text{ V}$ .

For constant scaled perturbation, the dependence of confinement time on plasma density is shown in Fig. 6. The data are well described by simple power laws for both the positive and negative perturbations. The best linear fits on the log-log graph have slopes of  $-1.45 \pm 0.06$  and  $-1.17 \pm 0.02$ , respectively. The confinement time of these asymmetric plasmas is approximately  $\tau_m^a(\text{scaled}) \propto n_p^{-1.3}$ ; the exponent,  $-1.3$ , is a rough approximation. In reality, the exponent may have some dependence upon  $V_p$ .

## VI. PLASMA LENGTH SCALING

The dependence of  $\tau_m^a$  on plasma length,  $L_p$ , is not clear. We attempted to determine the length scaling relations by measuring  $\tau_m^a$  for a wide range of perturbation strengths and plasma lengths. At each length, we used the standard  $\mathcal{C} V_p^{-2}$  scaling to determine the multiplicative constant  $\mathcal{C}$  for this length. Then we normalized the lifetime to a perturbation voltage of 5 V, and gathered all the different plasma lengths together onto the graph in Fig. 7. Unfortunately the irregularities in this data, shown in Fig. 7, prevent us from determining the length scaling.

## VII. MAGNETIC FIELD SCALING

The dependence of  $\tau_m^a$  upon the magnetic field,  $B$ , is remarkable because it does not follow the ubiquitous scaling,  $\tau_m \propto B^2$ , found in most symmetric traps.<sup>9</sup> The experimental data for asymmetric plasma confinement is shown in Fig. 8. While the scaling with magnetic field is of the

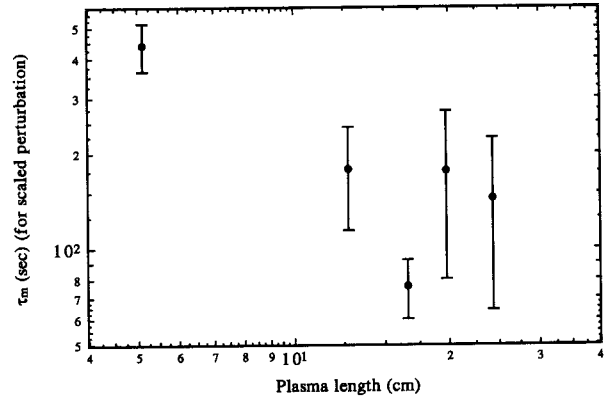


FIG. 7. Length dependence of asymmetric plasma confinement time.

form  $\tau_m^a \propto B^m$ ,  $m$  is measured to be  $0.45 \pm 0.06$  and  $0.80 \pm 0.04$  for the positive and negative perturbations, respectively. Regardless of the exact value of the exponent, the exponent is clearly different from the value  $m=2$ , obtained from symmetric traps. Thus the loss mechanism appears to be different for the large asymmetries studied here compared to the intrinsic construction asymmetries.

## VIII. CONCLUSION

The above scaling laws have been determined by varying each parameter while holding the other parameters constant. Assuming that the individual scaling laws remain valid when multiple parameters are varied, the individual scaling laws can be combined into one equation:

$$\tau_m^a \propto (n_p)^{0.7} (B)^{0.65} (T)^0 (V_p)^{-2}. \quad (2)$$

However, the required "separability" is not guaranteed. Here the density scaling is for the actual perturbation,  $V_p$ , rather than the scaled perturbation used in Sec. V. These scaling laws cannot be generalized to the case of  $V_p=0$  because each of the independent scaling laws was determined for  $|V_p| > 10 \text{ V}$ . Because of the unusual magnetic field scaling, the plasma loss mechanism appears to be in a different regime than in the standard, unperturbed case.

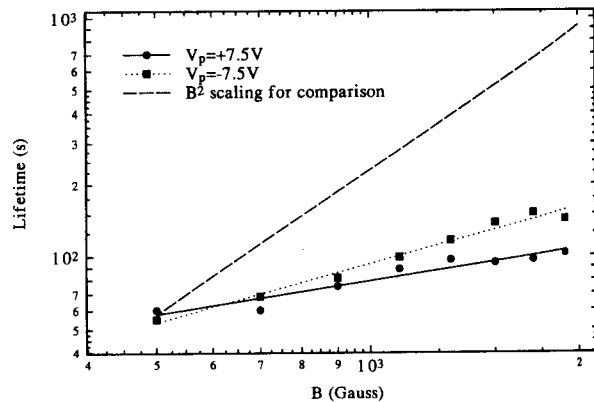


FIG. 8. Magnetic field dependence of asymmetric plasma confinement time.

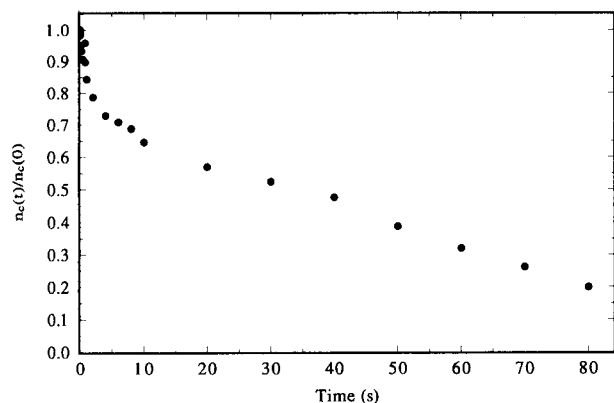


FIG. 9. Time evolution of plasma central density under the influence of perturbations. Note the two distinct time scales.

## APPENDIX: TIME EVOLUTION OF ASYMMETRIC PLASMAS

Following standard practice,<sup>7</sup> the confinement times measured in this paper are determined from the time for the central density,  $n_c$ , to be reduced by a factor of 2. The decay of  $n_c$  over time, however, is somewhat more complicated for these asymmetric plasmas than for symmetric plasmas. Most notably, there is an initial period of anomalously rapid reduction in  $n_c$ . The time scale of this dropoff is defined to be  $\tau_1$  and is typically 0.3 s. The amount by which the central density decreases during this stage is usually less than 20%. The remainder of the central density dropoff is more gradual, being described by a time constant,  $\tau_2$ , which can be hundreds of seconds. (In the case of high density, hot plasmas this initial, rapid dropoff is observed even without applied asymmetries.) Figure 9 shows the distinction between the two stages of plasma expansion. In many cases the  $\tau_1$  effect is negligible, and the plasma confinement time  $\tau_m^a$  is synonymous with  $\tau_2$ . In the previous sections, the early time behavior is discarded, and the measured confinement is equivalent to  $\tau_2$ .

This two-staged behavior has been observed by replacing the charge collectors with a phosphor screen<sup>20</sup> so the entire plasma can be imaged. During the  $\tau_1$  stage, the plasma radius is observed to expand rapidly without loss of total charge. The expansion slows down as the plasma approaches the chamber walls and the separatrix which lies between the closed and unclosed equipotential contour lines.<sup>10</sup> The remainder of the plasma evolution can be characterized by the slow reduction of central density and total charge as plasma is lost to the walls with a time constant  $\tau_2$ . The images indicate that during this phase, the density decreases uniformly with only slight changes in plasma radius.

Formally,  $\tau_1$  is defined as the time for  $n_c$  to drop half-way from its initial value to the point where there is an obvious "knee," that is, a point the  $\tau_2$  behavior takes over. There are some obvious difficulties with this definition. Most importantly, for small  $V_p$ , the division between  $\tau_1$

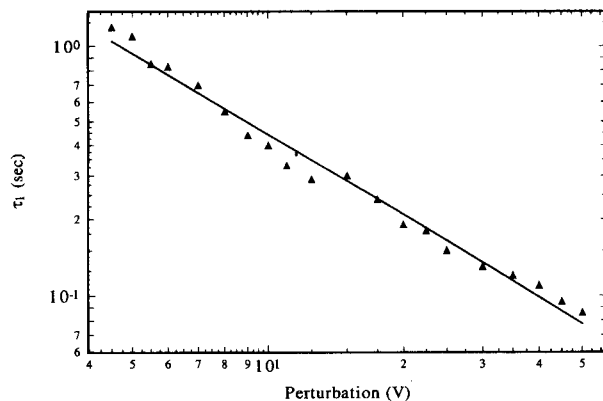


FIG. 10. Scaling of  $\tau_1$  with applied perturbations.

and  $\tau_2$  becomes artificial; there is just one smooth decay from the initial value of  $n_c$  to zero. Nevertheless, we have attempted to document the dependence of  $\tau_1$  upon the patch bias,  $V_p$ . Figure 10 shows that this dependence is fairly regular over an order of magnitude in  $V_p$ . With smaller biases, the  $\tau_1$  effect is not discernible, and for larger biases, the plasma shows evidence of being trapped by the wall patch as described earlier. The best fit to the data suggests that  $\tau_1 \propto |V_p|^{-1.1 \pm .03}$ . The amount of the initial dropoff also depends on the amplitude of  $V_p$ , but this behavior is not regular. The only conclusive statements that can be made is that the dropoff increases with increasing magnitude of  $V_p$ , and that positive perturbations cause a larger dropoff than negative perturbations.

<sup>1</sup>J. H. Malmberg, C. F. Driscoll, B. Beck, D. L. Eggleston, J. Fajans, K. Fine, X. P. Huang, and A. W. Hyatt, in *Nonneutral Plasma Physics*, edited by C. Roberson and C. Driscoll (American Institute of Physics, New York, 1988), Vol. 175, p. 28.

<sup>2</sup>R. C. Davidson, *Physics of Nonneutral Plasmas* (Addison-Wesley, Redwood City, 1990).

<sup>3</sup>G. Dimonte, *Phys. Rev. Lett.* **46**, 26 (1981).

<sup>4</sup>D. J. Heinzen, J. J. Bollinger, F. L. Moore, W. M. Itano, and D. J. Wineland, *Phys. Rev. Lett.* **66**, 2080 (1991).

<sup>5</sup>C. M. Surko, A. Passner, M. Leventhal, and F. J. Wysocki, *Phys. Rev. Lett.* **61**, 1831 (1988).

<sup>6</sup>T. M. O'Neil, *Phys. Fluids* **23**, 2216 (1980).

<sup>7</sup>J. H. Malmberg and C. F. Driscoll, *Phys. Rev. Lett.* **44**, 654 (1980).

<sup>8</sup>J. S. DeGrassie and J. H. Malmberg, *Phys. Fluids* **23**, 63 (1980).

<sup>9</sup>C. F. Driscoll and J. H. Malmberg, *Phys. Rev. Lett.* **50**, 167 (1983).

<sup>10</sup>J. Notte, A. J. Peurrung, J. Fajans, R. Chu, and J. Wurtele, *Phys. Rev. Lett.* **69**, 3056 (1992).

<sup>11</sup>R. Chu, J. S. Wurtele, J. Notte, A. J. Peurrung, and J. Fajans, *Phys. Fluids B* **5**, 2378 (1993).

<sup>12</sup>S. A. Prasad and T. M. O'Neil, *Phys. Fluids* **22**, 278 (1979).

<sup>13</sup>R. H. Levy, *Phys. Fluids* **8**, 1288 (1965).

<sup>14</sup>A. J. Peurrung, J. Notte, and J. Fajans, *Phys. Rev. Lett.* **70**, 295 (1993).

<sup>15</sup>J. Fajans, *Phys. Fluids B* **5**, 3127 (1993).

<sup>16</sup>W. D. White, J. H. Malmberg, and C. F. Driscoll, *Phys. Rev. Lett.* **49**, 1822 (1982).

<sup>17</sup>K. S. Fine, C. F. Driscoll, and J. H. Malmberg, *Phys. Rev. Lett.* **63**, 2232 (1989).

<sup>18</sup>D. L. Eggleston, *Bull. Am. Phys. Soc.* **37**, 1416 (1992).

<sup>19</sup>This assumption is motivated by the fact that the plasma is not in physical contact with the walls. Any asymmetries in the confining cylinders are communicated to the plasma through the asymmetric electric field produced by these asymmetries.

<sup>20</sup>A. J. Peurrung and J. Fajans, *Rev. Sci. Instrum.* **64**, 52 (1993).